



ELSEVIER

Available online at [www.sciencedirect.com](http://www.sciencedirect.com)

SCIENCE @ DIRECT®

E C E R S

Journal of the European Ceramic Society xxx (2005) xxx–xxx

[www.elsevier.com/locate/jeurceramsoc](http://www.elsevier.com/locate/jeurceramsoc)

## Phase diagram of high $T_c$ $\text{Pb}(\text{In}_{1/2}\text{Nb}_{1/2})\text{O}_3\text{--PbTiO}_3$ ceramics

C. Augier<sup>a,b,\*</sup>, M. PhamThi<sup>a</sup>, H. Dammak<sup>b</sup>, P. Gaucher<sup>b</sup>

<sup>a</sup> *Thales Research and Technology France, 91404 Orsay Cedex, France*

<sup>b</sup> *CNRS-UMR 8580 Ecole Centrale Paris, Laboratoire Structures, Propriétés et Modélisation des Solides, Grande Voie des Vignes, 92295 Châtenay-Malabry Cedex, France*

### Abstract

Dense  $(1-x)\text{Pb}(\text{In}_{1/2}\text{Nb}_{1/2})\text{O}_3\text{--}x\text{PbTiO}_3$  (PIN–PT) ceramics were synthesised by hot forging and thermal grain growth.  $(1-x)\text{PIN--}x\text{PT}$  phase diagram was investigated by X-ray diffraction and dielectric measurements. The morphotropic phase boundary zone was found to be between a rhombohedral phase region for low PT contents and a tetragonal phase region for high PT contents, i.e. in the 0.34–0.39 $x$  range. A mixture of tetragonal and probably monoclinic phases was observed for  $x=0.37$  at room temperature.

© 2005 Published by Elsevier Ltd.

**Keywords:** Powder-solid state reaction; X-ray methods; Dielectric properties; Pérovskite; Structural transition temperatures

### 1. Introduction

Lead-based relaxor ferroelectric solid solution ceramics with  $(1-x)\text{Pb}(\text{B}_1\text{B}_2)\text{O}_3\text{--}x\text{PbTiO}_3$  ( $\text{B}_1 = \text{Mg, In, Sc, Yb}$ ;  $\text{B}_2 = \text{Nb, Ta}$ ) formula exhibit excellent dielectric and electromechanical properties, especially at compositions near the morphotropic phase boundary (MPB). Such complex perovskites are of greater interest for piezoelectric actuators, underwater and medical transducers.

$(1-x)\text{Pb}(\text{Mg}_{1/3}\text{Nb}_{2/3})\text{O}_3\text{--}x\text{PbTiO}_3$  (PMN–PT) solid solution offers a large set of ferroelectric/piezoelectric properties and exhibits Curie temperature ( $T_c$ ) values from 120 to 170 °C depending on the composition. These low  $T_c$  prevent the use in more general applications. It has been reported that the system of  $(1-x)\text{Pb}(\text{In}_{1/2}\text{Nb}_{1/2})\text{O}_3\text{--}x\text{PbTiO}_3$  (PIN–PT) near its MPB ( $x=0.37$ ), which separates the pseudo-cubic and tetragonal phases, presents a high Curie temperature  $T_c \sim 300\text{ °C}^2$  and therefore potential for similar applications.

This paper reports a new study of the PIN–PT phase diagram. Three compositions: 0.68PIN–0.32PT, 0.63PIN–0.37PT and 0.58PIN–0.42PT have been studied by

X-ray diffraction to highlight the structural ferroelectric transitions when increasing the temperature. The phase transition temperatures were compared with the anomalies temperatures observed in the dielectric constant curves.

### 2. Experimental procedures

PIN–xPT perovskite powders were synthesised by solid state reaction via Wolframite method. Wolframite phase oxide ( $\text{InNbO}_4$ ) was formed at 1100 °C for 24 h. The perovskite powder, calcined at 850 °C for 2 h, was then pressed into pellets and hot-forged at 1000 °C for 1 h with a pressure of 1 T/cm<sup>2</sup>. The hot-forged ceramics were finally annealed under a  $\text{O}_2$  flow at 1200 °C for 4 h. Yellow pale translucent ceramics with high densities (>98%) were achieved.

PIN–PT poled discs were milled in liquid nitrogen for powder X-ray diffraction. The X-ray experiments were performed on a high-accuracy two-axes diffractometer using Cu  $\text{K}\beta$  monochromatic radiation issued from a Rigaku rotating anode (RU300, 18 kW). Selected regions of the diffractogram containing the (1 1 1), (0 0 2), (0 2 2) and (2 2 2) peaks were recorded and then fitted with Topaze™ Software to determine the peaks position and to calculate the lattice parameters.

\* Corresponding author. Tel.: +33 1 41 13 15 84; fax: +33 1 41 13 14 37.  
E-mail addresses: [augier@spms.ecp.fr](mailto:augier@spms.ecp.fr),  
[christophe.augier@thalesgroup.com](mailto:christophe.augier@thalesgroup.com) (C. Augier).

### 3. Results and discussion

Fig. 1 presents X-ray diffraction spectra of PIN-*x*PT compositions.

At room temperature, X-ray patterns show clearly that 0.58PIN-0.42PT exhibits a tetragonal phase characterised by a doublet of the (200) reflection and a singlet of the (111) one (Fig. 1a).<sup>4</sup> With increasing the temperature, the two peaks of the (200) reflection become closer and form at  $T_c = 330^\circ\text{C}$  a single peak characteristic of the cubic phase. The temperature dependence of the tetragonal and cubic lattice parameters is represented in Fig. 2a. At room temperature, the lattice parameters of the tetragonal phase are  $a_T = 4.022 \text{ \AA}$  and  $c_T = 4.132 \text{ \AA}$ .

For 0.68PIN-0.32PT, X-ray patterns obtained at room temperature show that (200) reflection is large and symmetric whereas (111) is large and presents a shoulder on the left side (Fig. 1b). Reticular distances deduced from (111), (200) and (220) reflections suggest that the ferroelectric phase at room temperature is rhombohedral. With increasing the temperature, (111) becomes symmetric and (200)

presents a shoulder on the left side at  $T > 190^\circ\text{C}$ , showing that a rhombohedral-tetragonal phase transition occurs at  $T_{RT} \sim 190^\circ\text{C}$  (Fig. 2b).

For PIN-0.37PT, the tetragonal phase is clearly observed between  $150^\circ\text{C}$  and  $T_c$  (Fig. 1c). At room temperature, (200) and (222) reflections are large and present several shoulders. (200) reflection presents three well-defined peaks whereas (222) reflection presents a diffuse shoulder on the left side. Two different hypotheses can be considered. First, a mixture between a tetragonal phase and a rhombohedral phase: the rhombohedral phase would be responsible for peak 3 and the tetragonal phase for peaks 1 and 2 of the (200) reflection. Then, a mixture between a tetragonal phase and a monoclinic phase: peak 1 would be indexed as  $(002)_T$ , peak 2 should be the superposition of  $(020)_M$  and  $(200)_T$  reflections and peak 3 should be the superposition of  $(002)_M$  and  $(200)_M$  reflections. By comparing these results with those obtained on the morphotropic compositions of PSN-PT,<sup>5</sup> PMN-PT<sup>6,7</sup> and PZN-PT,<sup>8</sup> this latter hypothesis seems to be the most probable. A Rietveld analysis is necessary to clearly identify the low-temperature phase. On the other hand, with increasing

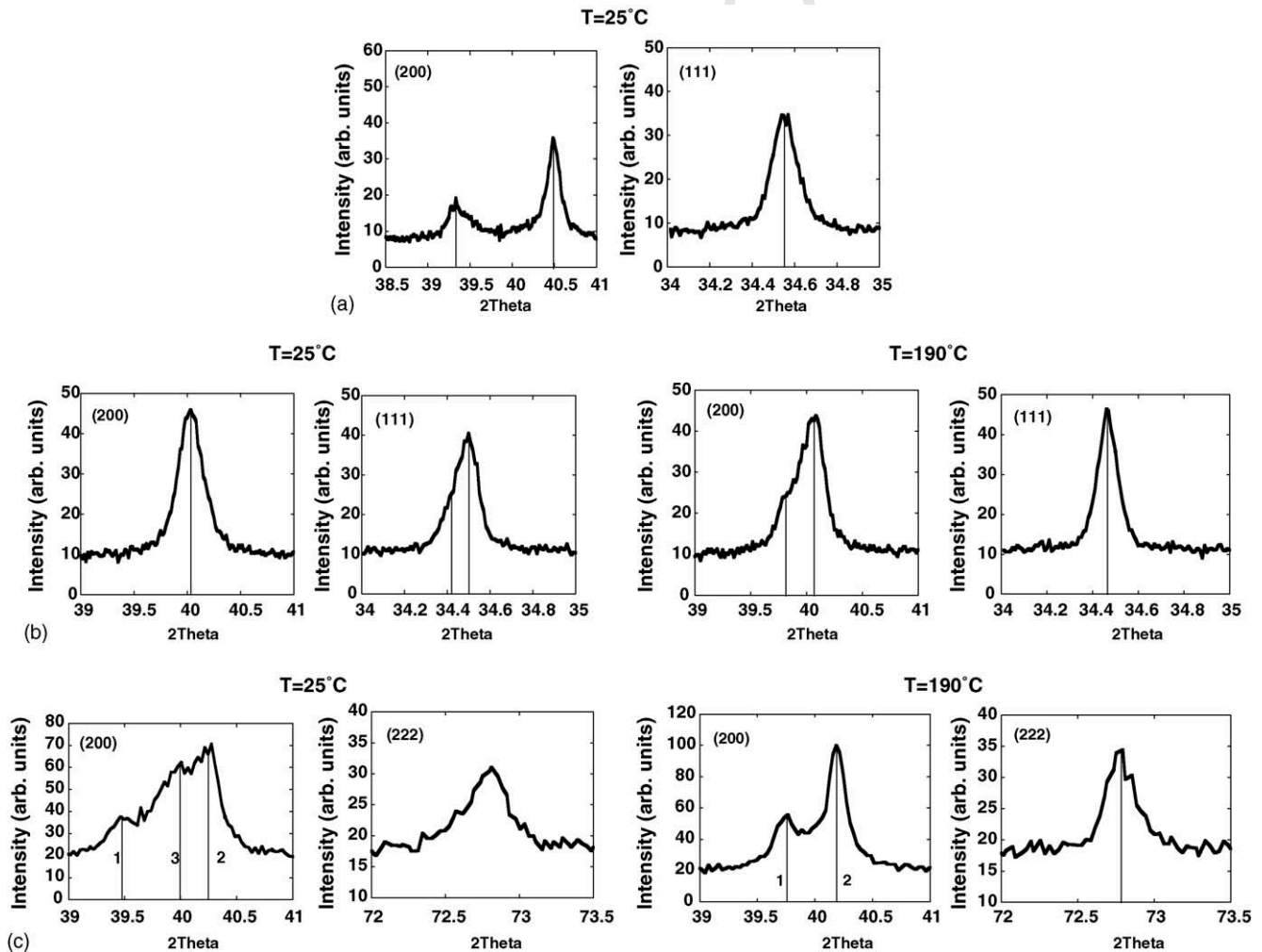


Fig. 1. (200), (111) and (222) peaks of 0.58PIN-0.42PT (a), 0.68PIN-0.32PT (b) and 0.63PIN-0.37PT (c) at  $T = 25$  and  $190^\circ\text{C}$ .

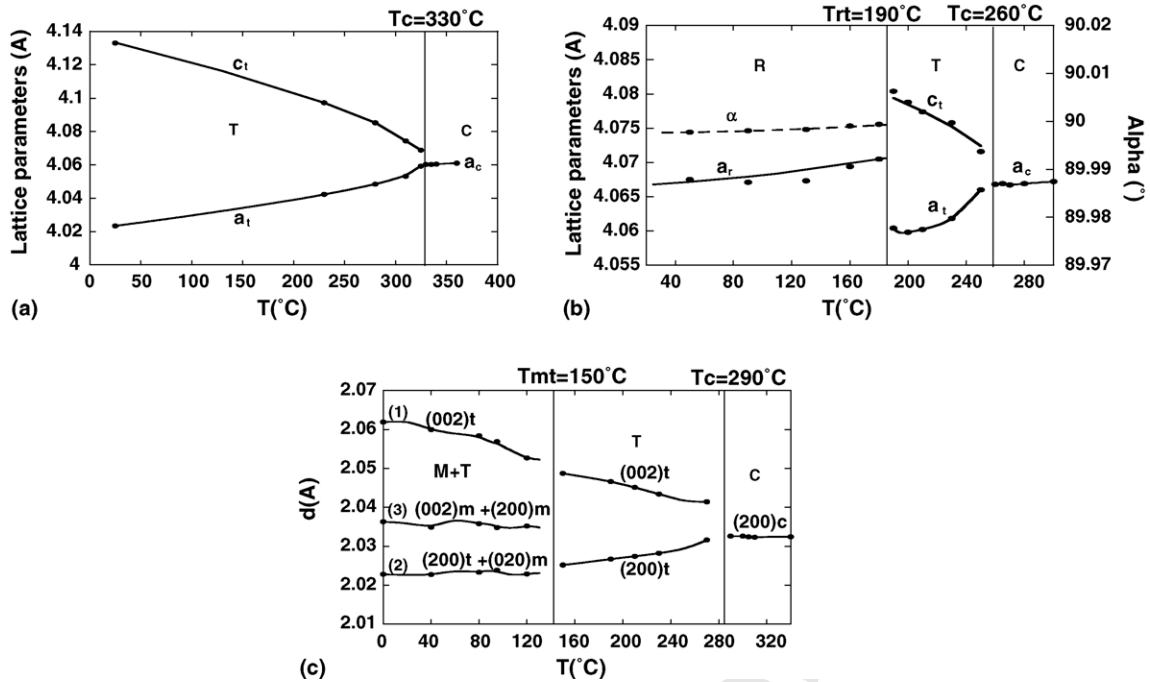


Fig. 2. Temperature dependences of the 0.58PIN–0.42PT (a) and 0.68PIN–0.32PT (b) lattice parameters and 0.63PIN–0.37PT (2 0 0) peak interplanar distance (c).

99 the temperature, the intensity of peak 3 decreases and vanishes at  $T_{MT} \sim 150^\circ\text{C}$  showing the monoclinic–tetragonal  
 100 phase transition. Fig. 2c represents the temperature depen-  
 101 dency of these (2 0 0) peaks reticular distances.  
 102

Fig. 3 shows the dielectric properties of  $(1 - x)\text{PIN}-x\text{PT}$  103  
 104 poled ceramics during a zero-field heating run (ZFH). The  
 105 dielectric curves, obtained at 1 kHz, present maxima at  $T_{\max}$   
 106 corresponding to the well known tetragonal–cubic phase tran-

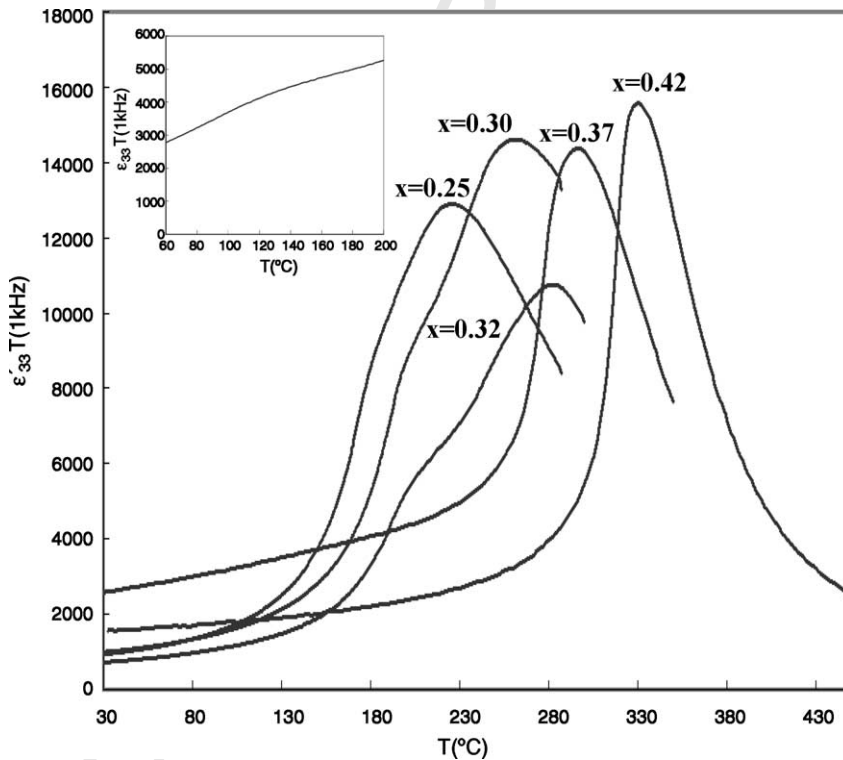


Fig. 3. Temperature dependence of the dielectric constant  $\epsilon'_{33} T$  at 1 kHz for different compositions of poled  $(1 - x)\text{PIN}-x\text{PT}$  ceramics.

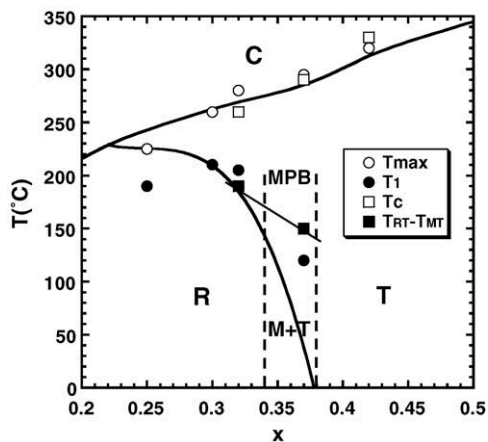


Fig. 4. Phase diagrams of  $(1-x)\text{PIN}-x\text{PT}$  system, solid line Alberta et al.<sup>2</sup>

sition. As expected,  $T_{\max}$  increases with  $x$  and remains between those of pure PIN and pure PT that are observed at 66 and 490 °C, respectively.<sup>2,3</sup> In addition the relaxor behaviour, which is observed for low values of  $x$ , disappears for  $x \geq 0.32$ .

For  $x=0.25$ , 0.30 and 0.32 the dielectric curves present another anomaly at a temperature  $T_1$  lower than  $T_{\max}$ . As shown above, this anomaly corresponds to the rhombohedral–tetragonal phase transition. This anomaly is less marked for  $x=0.37$  (cf. insert on Fig. 3) and non-existent for  $x=0.42$ .  $T_1$  seems to slightly vary around 200 °C for  $0.25 \leq x \leq 0.32$  and then decreases rapidly to  $\sim 120$  °C at  $x=0.37$ .

Fig. 4 represents in a diagram the structural transition temperatures determined by the dielectric study ( $T_{\max}$  and  $T_1$ ) and the X-ray diffraction study ( $T_c$ ,  $T_{RT}$  and  $T_{MT}$ ) as a function of the PT composition  $x$ . The dielectric and the X-ray results give comparable transition temperatures for  $x=0.32$ , 0.37 and 0.42. For  $x=0.25$  and 0.30, the presented dielectric results are coherent with those obtained previously in the same conditions by Alberta et al.,<sup>2</sup> whereas an important difference is observed for  $x=0.37$ . The low temperature transition occurs towards  $\sim 150$  °C instead of 20 °C as expected

according to their diagram. These results show that the morphotropic phase boundary is not described by a quasi-vertical line but by an extended region around  $x=0.37$ . This region is between a rhombohedral phase region for low PT contents and a tetragonal phase region for high PT contents.

#### 4. Conclusions

The X-ray study has revealed that the MPB zone of  $(1-x)\text{PIN}-x\text{PT}$  system separates a rhombohedral phase for low PT compositions from a tetragonal phase for high PT compositions. The composition near the MPB, 0.63PIN–0.37PT, has a  $T_c$  of 290 °C and presents a first structural transition from probably a monoclinic phase to a tetragonal phase at  $T_{MT} \approx 150$  °C.

#### Uncited reference

1.

#### References

- Hemery, H. Céramiques orientées hautes performances  $\text{Pb}(\text{Mg}_{1/3}\text{Nb}_{2/3})\text{O}_3\text{-PbTiO}_3$  par croissance interfaciale. Ph.D. thesis. Thales Research & Technology, France, December 2003.
- Alberta, E. F. and Bhalla, A. S., *J. Korean Phys. Soc.*, 1998, **32**, 1265–1267.
- Alberta, E. F. and Bhalla, A. S., *J. Phys. Chem. Solids*, 2002, **63**, 1759–1769.
- Planes were indexed using the pseudo-cubic axes.
- Haumont, R., Dkhil, B., Kiat, J. M., Al-Barakaty, A., Dammak, H. and Bellaiche, L., *Phys. Rev. B*, 2003.
- Kiat, J. M., Uesu, Y., Dkhil, B., Matsuda, M., Malibert, C. and Calvarin, G., *Phys. Rev. B*, 2002, **65**, 064106-1–4.
- Kumar Singh, A. and Pandey, D., *J. Phys. Condens. Matter*, 2001, **13**, 931–936.
- Renault, A. E., Dammak, H., Calvarin, G., Pham Thi, M. and Gaucher, P., *Jpn. J. Appl. Phys.*, 2002, **41**, 1–5.